Geomorphology 151-152 (2012) 207–223

Contents lists available at SciVerse ScienceDirect

Geomorphology

journal homepage: www.elsevier.com/locate/geomorph

Assessing the effect of sea-level change and human activities on a major delta on the Pacific coast of northern South America: The Patía River

Juan D. Restrepo A *

Department of Geological Sciences, EAFIT University, Medellín, Colombia, AA 3300
Teresa Lozano Long Institute of Latin American Studies, University of Texas at Austin, Austin, TX 78712, United States

ARTICLE INFO

Article history:
Received 24 June 2011
Received in revised form 1 February 2012
Accepted 5 February 2012
Available online 11 February 2012

Keywords:
South America
Patía River
Pacific coast
Delta geomorphology
River diversion
Relative sea-level

ABSTRACT

This paper presents the main physical and human-induced stresses that have shaped the recent evolution of the Patía River delta, the largest and best-developed delta on the western margin of South America. During the Holocene, the Patía Delta moved southward and the northern part became an estuarine system characterized by large extensions of mangrove ecosystems. However, a major human-induced water diversion, starting in 1972, diverted the Patía flow to the Sanguianga River, and shifted the active delta plain back to its former Holocene location. This discharge diversion has led to sediment starvation of the southern delta lobe and changed the northern estuarine system into an active delta plain. In addition, coastal areas of the Patía delta subsided as a result of a devastating tsunami in 1979. Morphological changes along the delta coast are evidenced by: (1) coastal retreat along the whole delta front during the period 1986–2001; (2) coastal retreat along the abandoned delta lobe for the period 2001–2008; 56% of the southern delta shoreline is retreating and only 4% of the coast shows signs of accretion; (3) progradation of the northern delta region during the period 2001–2008; the discharge diversion of the Patía River to the Sanquianga has apparently balanced the observed trends in coastal erosion and sea-level rise (5.1 mm yr^{-1} for the period 1984–2006, after the 1979 tsunami); (4) formation of transgressive barrier islands with exposed peat soils in the surf zone; and (5) abandonment of former active distributaries in the southern delta plain with associated inlet closure. In the northern delta lobe, major geomorphic changes include: (1) distributary channel accretion by morphological processes such as sedimentation (also in crevasses), overbank flow, increasing width of levees, inter-distributary channel fill, and colonization of pioneer mangrove; (2) freshening conditions in the Sanguianga distributary channel, a hydrologic change that has shifted the upper estuarine region (salinity < 1 psu) downstream; and (3) changes in vegetation succession; approximately 30% of mangrove forests in the current delta apex have been replaced by freshwater vegetation. Overall, the recent evolution of the Patía has been controlled by the interplay of (1) high basin-wide sediment load; (2) low discharge variability (Q_{max}/Q_{min}); (3) spatial switch of delta distributaries related to tectonic movements and subsidence; (4) a relative sea-level rise of 5.1 mm yr^{-1} after the occurrence of the 1979 tsunami; (5) episodes of sea-level rise associated with the ENSO cycle; and (6) human-induced discharge diversion. The information presented here is valuable evidence for understanding the role of extreme events versus 'normal' conditions in creating and shaping deltas.

1. Introduction

The coastline of a delta changes as a function of global eustasy (global ocean volume), regional earth-surface load changes (isostasic and tectonic factors), sediment supply, and compaction of the deposited sediment (Ericson et al., 2006). However, some deltas have seen the influence of eustatic sea-level change overwhelmed by the regional land-level signal (e.g., local and regional tectonic processes), which may be a more important control of delta development. Whereas subsidence increases the vulnerability of any given delta, the impact is made worse by anthropogenic control on the supply and routing of sediment to and across a delta (Ericson et al., 2006; Syvitski and Saito, 2007; Syvitski et al., 2009).

The consequence of delta subsidence, both natural of human-induced, in combination with discharge control, sediment-load reduction, and channel stabilization, is to accelerate shoreline erosion, threaten the health and extent of mangrove swamps and wetlands, increase salinization of cultivated land, and put human populations and coastal environments at risk (Syvitski et al., 2009). Under a subsidence scenario in any given delta, the system becomes less resilient to extreme events.

The morphology and recent evolution of the Pacific deltas of Colombia (Fig. 1) are unique compared to other South American deltas because of their singular combination of extreme climatic, geological, and

* Fax: +57 4 2664284.
E-mail address: jdrestre@eafit.edu.co.

0169-555X/$ – see front matter © 2012 Elsevier B.V. All rights reserved.
doi:10.1016/j.geomorph.2012.02.004

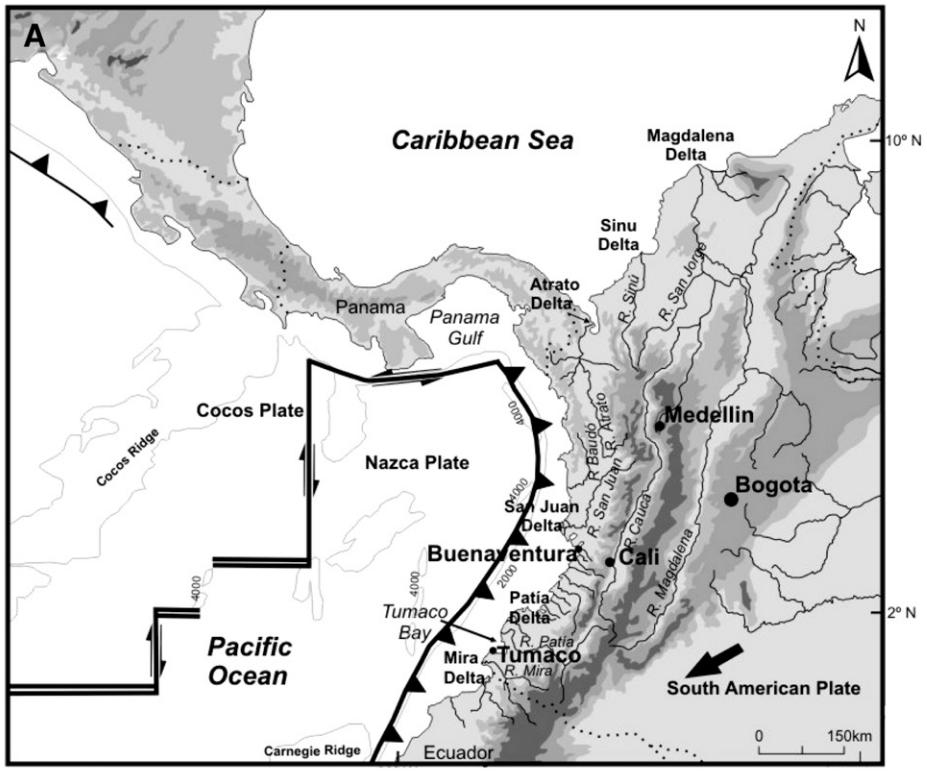
A
N
Caribbean Sea
Magdalena Delta
10° N
Sinu Delta
Atrato Delta
Panama
Panama Gulf
R. Sinú
R. San Jorge
Cocos Plate
Cocos Ridge
Nazca Plate
R. Baudó
R. Atrato
Medellin
R. San Juan
R. Cauca
Bogota
San Juan Delta
Buenaventura
Cali
R. Magdalena
Patía Delta
Tumaco Bay
R. Patía
Mira Delta
Tumaco
R. Mira
2° N
Pacific Ocean
South American Plate
Carnegie Ridge
Ecuador
0 150km

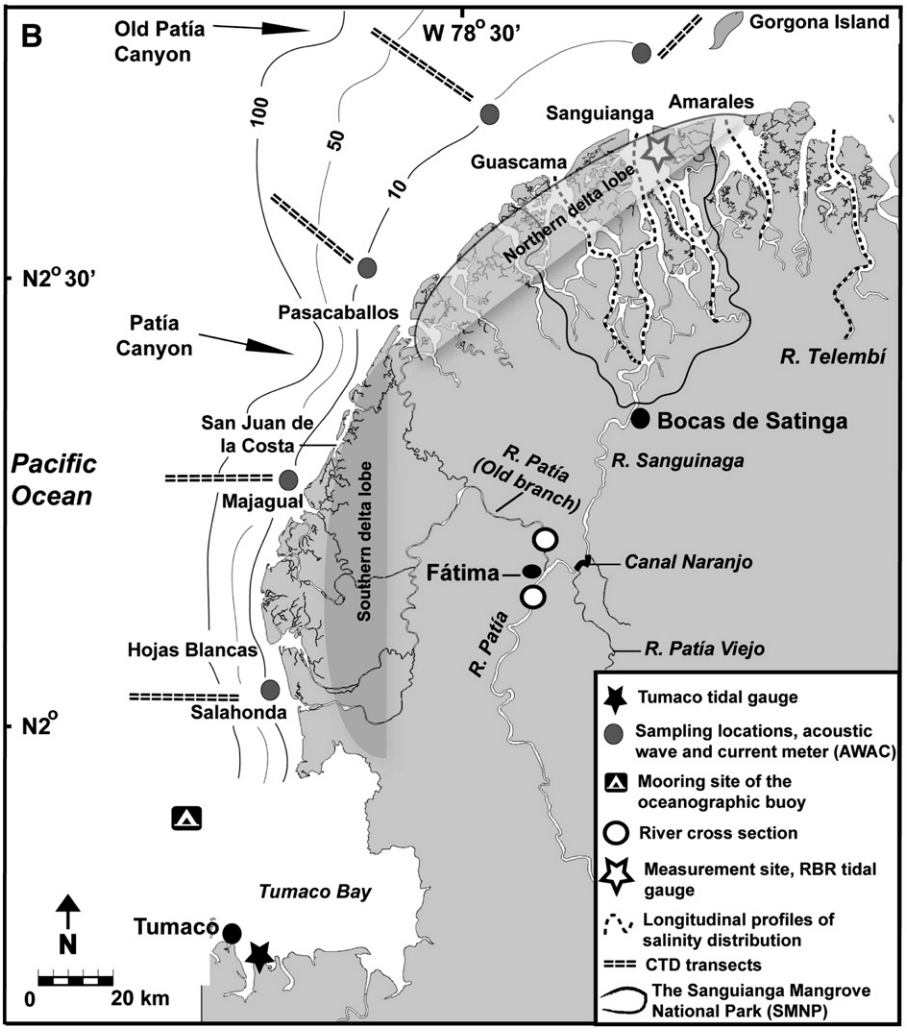
B
Old Patía Canyon
W 78° 30'
Gorgona Island
Sanguianga
Amarales
Guascama
Northern delta lobe
100
50
10
N2° 30'
Pasacaballos
Patía Canyon
R. Telembí
Bocas de Satinga
San Juan de la Costa
R. Sanguinaga
Pacific Ocean
R. Patía (Old branch)
Majagual
Southern delta lobe
Fátima
Canal Naranjo
R. Patía
R. Patía Viejo
Hojas Blancas
Salahonda
N2°
Tumaco Bay
Tumaco
N
0 20 km
Tumaco tidal gauge
Sampling locations, acoustic wave and current meter (AWAC)
Mooring site of the oceanographic buoy
River cross section
Measurement site, RBR tidal gauge
Longitudinal profiles of salinity distribution
CTD transects
The Sanguianga Mangrove National Park (SMNP)

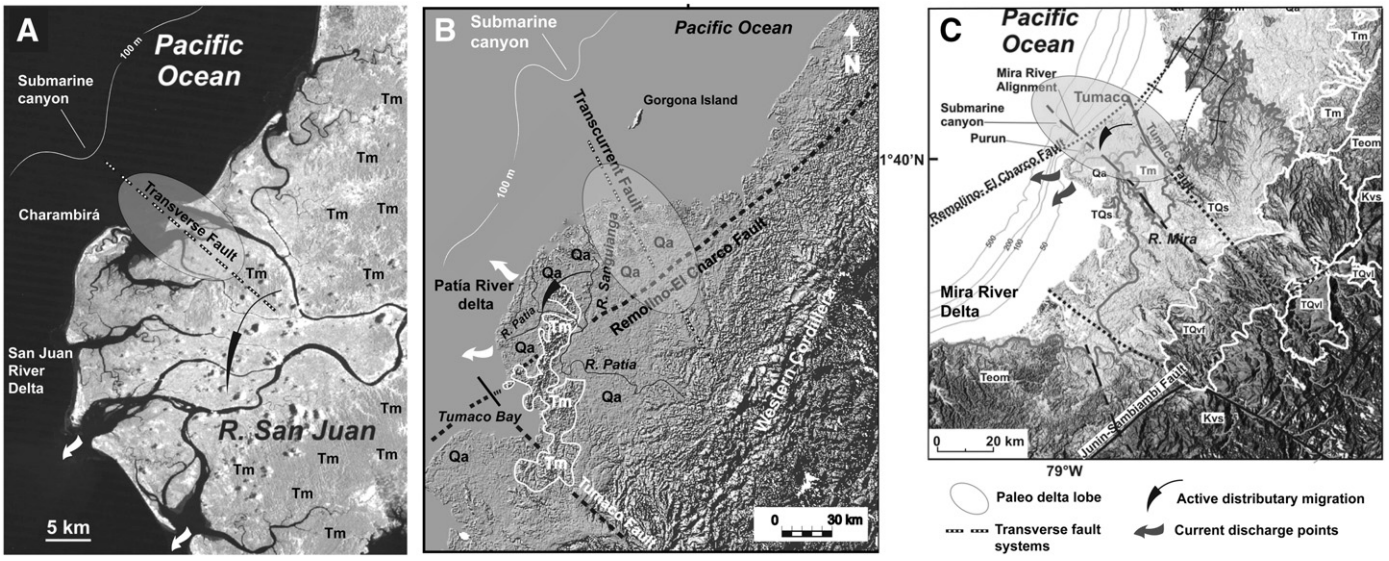

Fig. 2. Intera Radar image (A) and hillshade generated images from DEM data (SRTM, Shuttle Radar Topography Mission, 2002) (B–C) of the Pacific deltas of Colombia: (A) San Juan, (B) Patía and (C) Mira. We show the main tectonic features and geologic formations, including transverse paleofractures, submarine canyons, recent alluvial deposits (Qa), and Tertiary formations of marine Miocene rocks (Tm). Also, the spatial switch of delta distributaries related to tectonic movements, is shown.

oceanographic conditions in which the deltas are built, including (1) high tectonic activity with the occurrence of shallow earthquakes and tsunamis (Kellogg and Mohriak, 2001); (2) narrow continental shelves with limited accommodation space (Correa, 1996); (3) drainage basins that receive high rates of precipitation resulting in large quantities of water discharge and sediment load (Restrepo and Kjerfve, 2000); (4) the complexity of littoral dynamics resulting from mesotidal ranges (Restrepo and Kjerfve, 2002; Restrepo et al., 2002), and the effect of significant swells and associated coastal currents (Restrepo et al., 2002); (5) strong oceanographic manifestations associated with the ENSO cycle, causing episodic sea-level rises during El Niño years (Morton et al., 2000); and (6) increasing rates of relative sea-level rise (Restrepo et al., 2002; Restrepo and López, 2008). It is worth noting that small rivers form extensive deltas along the Colombian Pacific coast, despite the occurrence of highly energetic and destructive conditions.

The Patía River delta, the most extensive and well developed delta on the Pacific coast, measuring 1700 km^2 (Fig. 1), experienced a large tsunami in 1979. Coastal areas of the Patía delta, including San Juan de la Costa and the northern distributaries at Sanquianga (Fig. 1), subsided and experienced an apparent sea-level rise along at least a 200 km stretch of the Colombian coast north of the Ecuadorian border (Herd et al., 1992; Correa and González, 2000).

In addition to the tectonically-induced subsidence along the Patía River delta, a major water diversion, starting in 1972, diverted the Patía flow to the Sanguianga River; the latter being a small stream draining internal lakes from the Pacific lowlands (Fig. 1). This human-induced discharge diversion shifted the active delta plain back to the north, and changed the northern estuarine system into an active delta plain.

Although the scientific community of Colombia is aware of the physical changes occurring in the Patía River delta, there no studies have analyzed the impact of natural and anthropogenic drivers on the modern Patía delta development. This paper presents a preliminary view on how the main physical and human-induced stresses, including sea-level change and a major human-induced water diversion, have shaped the recent evolution of the Patía River delta. It analyzes the environmental consequences of sea-level change and the discharge diversion in terms of (1) delta lobe migration, (2) geomorphic changes along the delta front and distributary channels, and (3) ecological impacts on mangrove ecosystems.

2. The Patía River delta

The Patía River catchment with an area of 23,700 km^2 has the largest drainage basin of the Colombian rivers draining into the Pacific. The delta is characterized by high tectonic activity and progrades on a narrow shelf bordering a deep trench. Along the Colombian Pacific margin, the Nazca oceanic plate is converging with the South American continental plate at a rate of 54 mm yr^{-1} (Kellogg and Mohriak, 2001) (Fig. 1A). The convergence has produced an unstable coast characterized by the occurrence of large magnitude and shallow focus earthquakes.

Along the Patía delta front, more than 20 earthquakes with magnitude 4–6 occurred within 200 km of the shoreline from 1993 to 2007 (López et al., 2009). In addition, most intense earthquakes during the 20th century occurred in 1906 and 1979 (Pennington, 1981; Lockridge and Smith, 1984; Meyer et al., 1992; INGEOMINAS, 2007), and caused both regional and local subsidence. During the tsunami in 1979, coastal areas of the Patía delta subsided as much as 1.6 m (Herd et al., 1992).

In the Pacific deltas of Colombia there are no quantitative measurements of recent coastal subsidence to verify tectonic subsidence. However, limited qualitative evidence in the Pacific deltas suggests that subsidence is occurring in this part of the coast (Restrepo et al., 2002), including (1) the correspondence of increasing trend in relative sea level with tectonic setting, (2) the increased occurrence of non-storm washover events and earthquake activity, and (3) transgressive barrier islands with exposed peat soils on the beach front.

Deltaic river distributary channels often shifted episodically their location and pattern during the recent Holocene due to changes in

Fig. 1. (A) Map of the Pacific coast of Colombia, showing the locations of Colombian deltas and the tectonic setting of the Pacific active margin. (B) Map of the Patía River delta, showing the locations of: (1) the channel diversion site at Fátima, (2) southern and northern delta lobes, and (3) sampling locations of oceanographic and hydrologic measurements.

natural forces such as tectonic activity, relative sea-level, river fluxes, and tidal and wave energies; causing further aggradation of delta lobes (Syvitski et al., 2009). Along the Pacific coast of Colombia (Fig. 1A), the overall southward displacement of the main delta distributary channels has been associated with the presence of active transcurrent faulting associated with several transverse paleofracture zones (Gómez, 1986a, 1986b; Correa, 1996; González et al., 2002; Restrepo et al., 2002). Paleochannels indicate that delta distributaries have undergone rearrangements due to seismic events (Gómez, 1986a). Tectonic activity in the Pacific deltas of Colombia caused that most of the active distributaries switched their locations from northerly to southerly over the course of 50 decennia (Restrepo et al., 2002) (Fig. 2). However, distributary channel accretion in the northern Patía delta lobe during the last four decades indicates that the recent delta evolution has been controlled by human activities. Changes in water discharge and sediment load due to the water diversion in 1972 have reversed the overall southward shift of active distributaries. Thus the tectonic control is not the main driving mechanism of the current pattern of delta migration.

For the northern Patía River delta (Figs. 1B and 2B), remainders of a paleocanyon provide evidence that the active delta lobe shifted to the south 500 years ago (Correa, 1996) where it stayed until recently. The northern part became an estuarine system characterized by large extensions of mangrove ecosystems, little fresh water inflow and no significant fluvial sediment inflow from the western Andes. The Sanquianga Mangrove National Park (hereafter named SMNP) is the largest ecological reserve along the Pacific coast South America and is situated on this new Patía-Sanquianga delta plain (Fig. 1B).

The Patía delta experiences a semi-diurnal tide with an average tidal range of 1.9 m inside the distributary channels. The harmonic constants indicate that the mean tidal range in the Sanquianga distributary mouth (Fig. 1B) is 2.4 m, the fortnightly spring tidal range measures 2.9 m and the neap tidal range is 1.7 m. In the southern part of the delta at Pasacaballos inlet (Fig. 1B), the mean tidal range, fortnightly spring tidal range and neap tidal range are 2.4, 3.2 and 1.2 m, respectively. In addition, observed waves in the Patía delta are predominantly swells from the southwest, with a maximum significant height of 1.4 m and an average peak period of 14 s.

According to Restrepo and López (2008), the Patía delta is a tide-influenced system and exhibits definite characteristics of mixed wave and tide-influenced delta due to the interplay of (1) moderate wave conditions as a result of the effect of significant swells from the SW, (2) meso-tidal range, (3) a steep sub-aqueous profile, and (4) a low attenuation index of deep-water waves. As a result, marine hydrodynamic conditions of the Patía delta are one of the highest energy setting of all Colombian deltas, more comparable to the large deltas bordering the Atlantic ocean of South America such as the Orinoco and the Paraná deltas.

Fig. 3 shows the morphologic classification of Colombian deltas, including the Patía, done by using the quantitative relationships between log mean tidal range/mean wave height versus log suspended sediment load (Hori and Saito, 2007; Restrepo and López, 2008). When comparing the Patía Delta with worldwide similar deltas, the Patía belongs to tide-influenced delta type, similar to major deltas such as Fly, Mekong, Irrawaddy, Ganges–Brahmaputra, Changjiang and Amazon. These tide-influenced deltas, which are common along mesotidal and macrotidal shorelines, exhibit funnel-shaped river mouth morphology. Although the Patía Delta has a significant river-produced bulge, its shoreline has been smoothed into regular and rounded forms by wave activity (Fig. 1A). Continuous beach and beach-ridge formations fringe the coastline of this delta. An interesting feature arising from this classification scheme is the contribution of wave energy to the morphology of the Patía Delta. Even though the Patía is not classified as mixed wave- and tide-influenced delta, its coast has been intensely eroded and reworked by wave action.

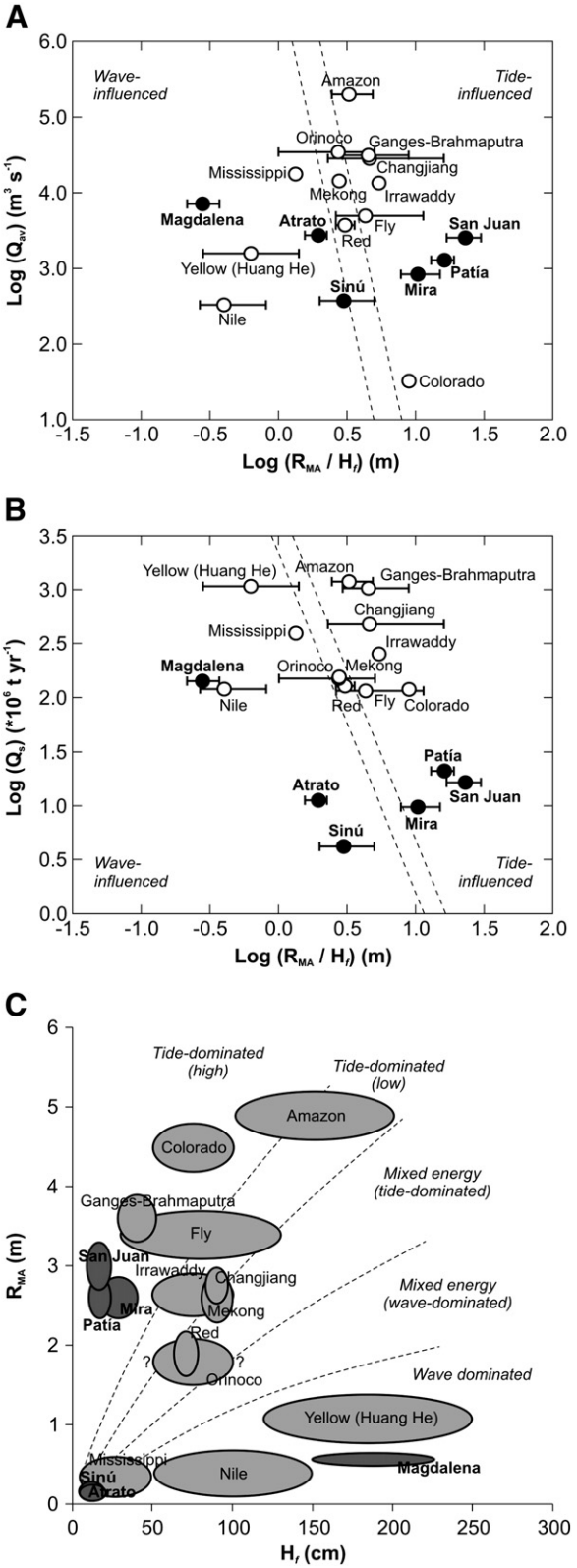

Fig. 3. Classification diagrams for major Colombian deltas plotting mean tidal range/mean wave height versus log water discharge (A) and log suspended sediment load (B). The dashed lines divide the three types of deltas, including wave-influenced (left side), mixed tide and wave-influenced (center), and tide-influenced deltas (right side). (C) Mean wave height versus mean tidal range for major Colombian deltas. The regions are grouped into five morphological categories (after Hori and Saito, 2007).

3. Material and methods

This study develops the geo-physical baseline information of the Patía delta, including (1) a summary of the hydrologic and geologic settings in which the delta was formed; (2) data and analyses of distributary mouth and coastal processes; (3) a hydrodynamic model upscaled to the entire delta system; (4) analysis of geologic processes in terms of shore dynamics and trends in relative sea level in the past century; and (5) further quantitative comparisons with Colombian and other major world deltas.

Daily water discharge and suspended sediment load data (1969–2003) were obtained at 4 sites along the Patía River from the Hydrological Institute of Colombia, IDEAM (IDEAM, 2009) (Fig. 6A). In addition, we took measurements of water discharge at two river cross-sections in the apex of the delta at Fátima during December 2009 (Fig. 1B).

The modern development of the Patía River delta was examined by analyzing different geological studies (Van Es, 1975; Gómez, 1986a, 1986b; Correa, 1996; Correa and González, 2000; Moreno, 2003), and by using a French Navy chart from 1875 and a local map from 1924.

To assess morphological changes along the delta front and distributary channels during the last four decades, after the channel diversion occurred in 1972, 30 m-pixel resolution Landsat 7 satellite images from 1986, 1987, 1996, 2001, obtained from the Global Land Cover Facility of the University of Maryland, and one 15 m-pixel Aster image from 2008, were processed. Detailed temporal analyses of distributary channel morphology at the diversion site and shoreline changes along the delta front were documented using aerial photographs from 1962 and 1986 at a scale of 1:40,000, topographic maps at a scale of 1:25,000, and through interviews with inhabitants.

To estimate rates of coastal retreat and progradation, the coastline was extracted from satellite images in 1986, 2001, and 2008 by using ISODATA and band ratio methods. Rates of coastline change were determined by using DSAS software, which estimates rate of change statistics from multiple historic shoreline positions residing in GIS (Thieler et al., 2009). DSAS transects were spaced 100 m apart and rates of shoreline change were calculated at each transect using linear regression applied to successive shoreline positions in 1986, 2001, and 2008.

To compare and contrast the physical changes occurring in the delta distributaries and associated environments, field observations were carried out along five main distributaries and their inlets, the Sanquianga, Guascama, Pasacaballos, Majagual and Salahonda (Fig. 1B). Also, longitudinal measurements of vertical profiles of conductivity and temperature were taken along the Sanquianga, Guascama and Amarales distributaries from the entrance to the apex at Bocas de Satinga, to obtain a quasi-synoptic characterization of the longitudinal salinity distribution and the corresponding vegetation association (Fig. 1B).

In addition, hourly sea-level data were obtained from the tidal gauge at Tumaco (1953–2006) (IDEAM, 2007) (Fig. 1B). The trend in relative sea level in the Patía Delta is estimated by least-squares linear regression for the Tumaco time series. To evaluate the monthly mean sea-level anomalies near the deltas related to ENSO, we removed mean monthly values to eliminate seasonal effects. A filtered sea level was calculated by subtracting the interannual mean sea level for each month (S^*) from the respective monthly mean sea level in each year (S) for the ith month of the jth year to form the deviation from the long-term monthly mean sea level $S_{ij} = S_{ij} - S_i^*$ (Quinn et al., 1978; Enfield and Allen, 1980). The Sea Surface Temperature anomaly (SST) data were obtained from the National Oceanic and Atmospheric Administration—NOAA.

To assess wave climate in the Patía River delta and provide a statistical description of the sea state, this study obtained wave data around the delta for the period 1979–2000 from the NOAA implementation of the third-generation wind-wave model WAVEWATCH III (NWW3) (Tolman, 2002). The data include 64,552 sets of predominant direction, significant wave height, and peak period. Also, this study obtained wave data along the delta front from the AWAC measurements (Fig. 1B), including significant and maximum wave heights, peak and mean periods, and wave direction.

To estimate changes in vegetation cover in the Sanquianga Mangrove Reserve (Fig. 1B), after the discharge diversion of the Patía River occurred in 1972, three Landsat satellite images for the period 1986–2001 were processed and classified. Classification categories were based on the scheme proposed by the Mangrove Assessment of the Southern Pacific Coast (Tavera, 2009), with some modifications. The resulting 13 spectral clusters were labeled and grouped into six major forest and non-forest cover categories, supported by secondary data analysis, including vegetation maps (1:250,000), black and white aerial photographs (scale 1:40,000), and by consulting previous vegetation classifications (e.g., Tavera, 2009). To validate and correct the resulting six major spectral categories, a supervised classification was carried out by visiting the Sanquianga Mangrove Reserve in 2009 and 2010.

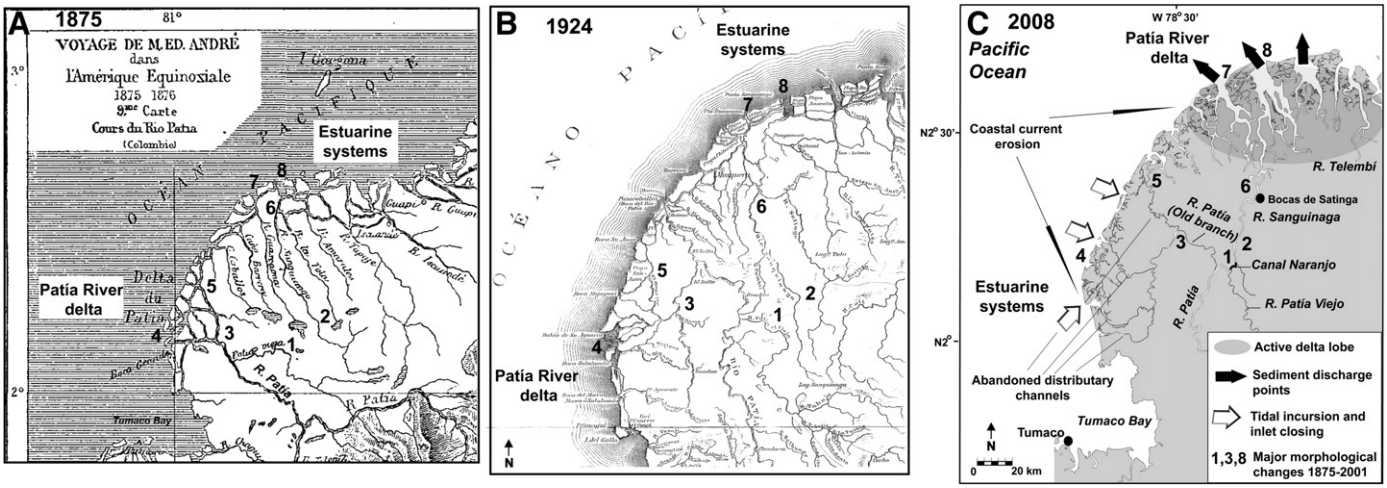

Fig. 4. Analysis of major morphological changes in the Patía delta from 1875 to 2008 based on a French Navy chart (1875) (A), a local map from 1924 (B), and an Aster image from 2008 (C).

4. Results

4.1. Modern Patía delta development

Analysis of delta morphology between 1875 and 2008 indicates major morphological changes during this 126-year period (Fig. 4A–C), including: (1) flow diversion from the Patía River to the Sanquianga River; (2) widening of the Sanquianga River; (3) narrowing of the Old Patía branch due to confined fluvial flows; (3) distributary channel abandonment at the former delta apex; (4) narrowing of inlets at the southern delta lobe, formation of ebb tidal deltas, and overall retreat conditions in the delta front; (5) coastline erosion at the former northern tributary, the Pasacaballos inlet; (6) active sedimentation at the new delta apex, Bocas de Satinga; and (7–8) migration of active fluvial discharge points from the southern delta lobe to the new active delta lobe. The barrier islands present in 1875 at Sanquianga and Amarales were accreted to the main delta lobe. Also, there is an evident widening of active distributary channels and overall frontal accretion of the Sanquianga River mouth (Fig. 4A).

As mentioned before, geologic evidence indicates that the active Patía delta lobe shifted to the south in the Quaternary, as a result of tectonic activity (Fig. 2B). Since then, the accreting delta front has been located in the southern portion of the delta plain. The northern part became an estuarine system characterized by large extensions of mangrove ecosystems (Fig. 1B), little fresh water inflow and no significant fluvial sediment load from the western Andes. However, most of the Patía's fluvial flux was diverted to the Sanquianga River

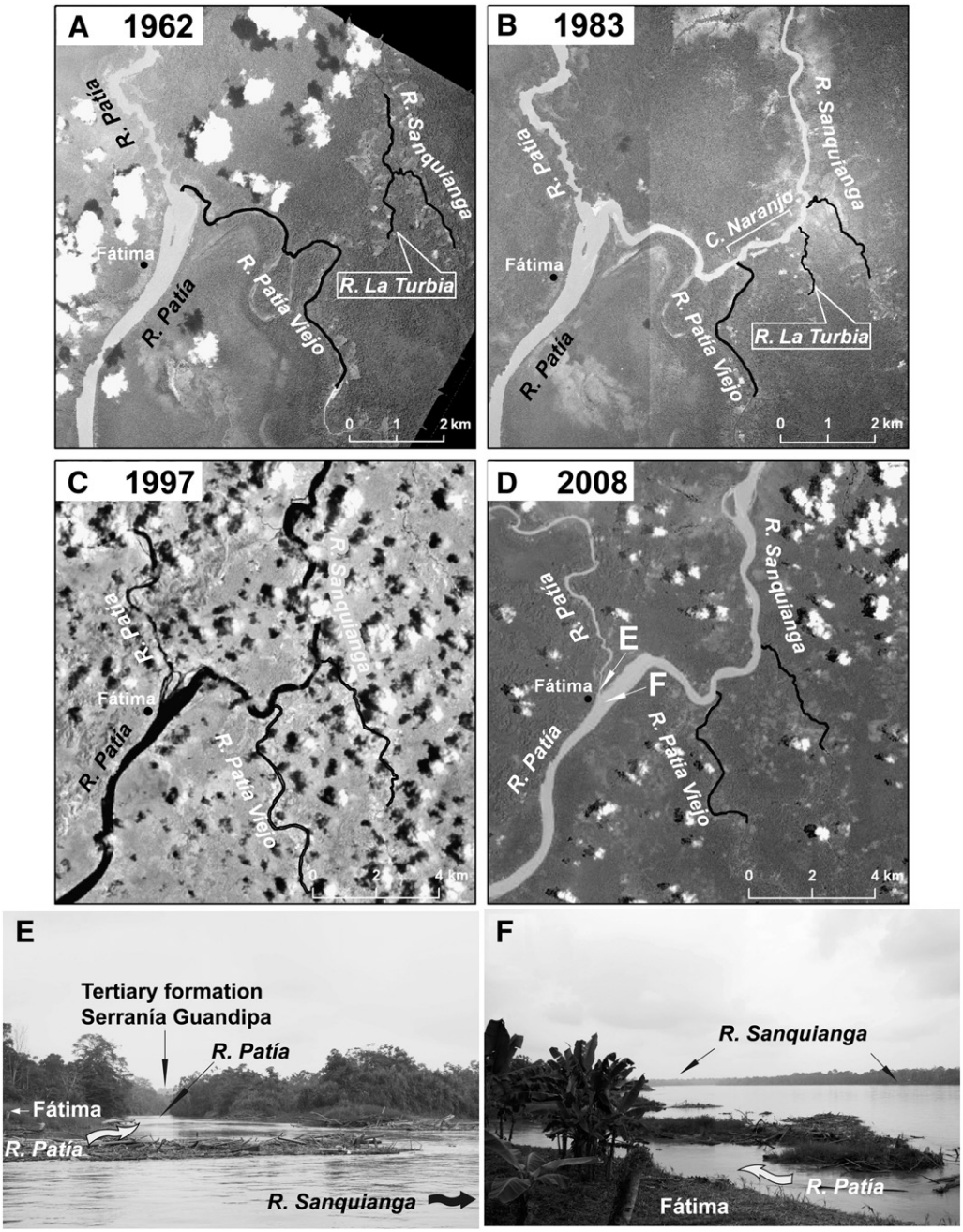

Fig. 5. Aerial photographs 1962–1983 (A–B), Landsat satellite image 1997 (C), and Aster image from 2008 (D), showing major morphological changes at the channel diversion site. Observe the widening process of the Sanquianga River and the confined flow of the Patía. (E–F) Diversion site at Fátima (Fig. 1B), showing the current confined flow through the Patía River and the channel width of the Sanquianga.

in 1972 and shifted the active delta plain back to its former location. A wood merchant constructed a 3 km-long channel (Canal Naranjo), which was dredged to connect the Patía Viejo tributary with the much smaller Sanquianga River to the north (Figs. 1B and 5B). Prior to the construction of the Canal Naranjo in 1972, the Patía Viejo distributary channel joined the Patía River at Fátima and the whole Patía River discharge flowed to Salahonda (Fig. 1B). Nowadays, more than 90% of the Patía River discharge has been redirected through the Canal Naranjo – Patía Viejo tributary – to the Sanquianga River system. This discharge diversion left the southern delta plain under a regime of sediment starvation and reduced fluvial flows.

Fig. 5 shows the morphological variations of the Patía and Sanquianga rivers at the diversion site. In 1962 (Fig. 5A), there was no connection between the two rivers and the Patía Viejo was an active and meandering distributary channel. In 1983 (Fig. 5B), after the Canal Naranjo was excavated, the Patía migrated towards the Sanquianga River. At this time, the Patía Viejo was an active branch with flow connection to the Sanquianga River. In 1997 (Fig. 5C), the Patía River showed less hydraulic capacity and sediment accumulation created elongated bars at the entrance to the Patía River (Fig. 5E–F). The new branch, now formed by the Patía and Sanquianga, named Patianga in the region, became a large river (Fig. 5D–F). Currently, the Patianga transports nearly all water discharge and its width is of the same magnitude as the former Patía River width.

4.2. Water discharge and sediment load into the active delta plain

Based on daily stage measurements from 1969 to 2003, the Patía River as gauged at Puente Pusmeo (Fig. 6A) discharges on average 10 $km^3\,yr^{-1}$, with a seasonal root mean square (rms) of 3 $km^3\,yr^{-1}$. Peak flows exceeding 14 $km^3\,yr^{-1}$ were observed during La Niña years 1973, 1984, and 2000, while low discharges below 9 $km^3\,yr^{-1}$ were observed during El Niño years 1972 and 2001 (Fig. 6B). The mean river discharge flowing into the delta plain is 42 $km^3\,yr^{-1}$ because of the large contribution of the Telembí River, the last tributary before the delta (Fig. 6A).

Rainforest rivers show high but variable peak discharges during the rainy season. Similar to other world rainforest rivers, Andean rivers of Colombia display two annual flood peaks, in agreement with bimodal distribution of rainy periods in summer (main) and fall (secondary). However, when analyzing discharge variability for world tropical rivers in different hydrologic and morphoclimatic zones, Colombian rivers, including the Patía, show the lowest values of Q_{max}/Q_{mean} and Q_{max}/Q_{min} ratios compared to other rainforest rivers (Fig. 6C). Thus, the Patía River is a high runoff system with low discharge variability and more water available for hillslope erosion and sediment transport.

Our measurements of water discharge at the Patía River cross-section during December 2009 (Fig. 1B) show that the average water discharge before the diversion site in Fátima was 1100 $m^3\,s^{-1}$. Further measurements indicate that a small fraction of water discharge, only 84 $m^3\,s^{-1}$ flows to the old Patía branch. Thus, the Sanquianga River carries almost the whole Patía River flow. It is worth noting that measurements were taken at the beginning of rising levels in December, a period that coincides with the rainy season in the Patía River drainage basin.

Based on daily sediment load data from 1972 to 2001 by IDEAM (Fig. 6B), sediment loads from the upper river measure 0.92, 16.2, and 13.9×10^6 t yr^{-1}, as gauged at La Fonda, Puente Guascas, and Puente Pusmeo, respectively (Fig. 6A). The corresponding sediment yield ranges from 477 t $km^{-2}\,yr^{-1}$ at La Fonda to 1715 t $km^{-2}\,yr^{-1}$ at Puente Pusmeo for the most downstream portion of the river (Fig. 6A). The latter yield, which represents 60% of the whole catchment area, does not exhibit the conditions of deposition and storage that occur in the entire basin. To remedy this, we further estimated sediment load for the non-gauged area of the Patía River from the regression of sediment yield on basin area from gauged stations. The mean sediment yield for the watersheds of Telembí and Magui rivers are 620 t $km^{-2}\,yr^{-1}$ and 355 t $km^{-2}\,yr^{-1}$, respectively. Our best estimate of sediment load into the active delta plain at Bocas de Satinga (Fig. 1B) from both gauged and non-gauged Patía distributaries is 27 Mt yr^{-1}. This results in a sediment yield of 1500 t $km^{-2}\,yr^{-1}$ (Fig. 6A).

4.3. Relative sea-level change

The trend in relative sea level was estimated by least-squares linear regression for the Tumaco 1953–2006 time series (Figs. 1B and 7B). In Tumaco the relative sea-level rise measured -0.6 mm yr^{-1} in the period 1953–2006, indicating a decreasing trend in sea level for this 53 yr-period. However, an increasing trend in relative sea level of 5.1 mm yr^{-1} is observed for the period 1984–2006, after the occurrence of the 1979 tsunami (Lockridge and Smith, 1984; Meyer et al., 1992) (Fig. 7B). Sea-level data for the 1982–1983 El Niño event was removed from the 1984–2006 short-term trend analysis since this eustatic signal adds some noise to the observed isostatic trend after the occurrence of the tsunami.

At Tumaco (Fig. 1B), high sea-level anomalies and the Southern Oscillation Index (SOI) show good correspondence with the 53-year period 1953–2006 (Fig. 7C–D). Regression analysis between the smoothed sea level and the smoothed SOI yielded a coefficient of determination of $R^2 = 0.61$, a coefficient significant at the 95% confidence level. This indicates that variations in the SOI explain 61% of the seasonal variability in water level, with low values of SOI corresponding to high Tumaco sea-level anomalies. Hence, the sea level in the Patía delta is strongly affected by the Southern Oscillation.

As a result of relative sea-level rise (Fig. 7B), transgressive barrier islands are present along the Patía delta front (Figs. 7E–H). These islands appear to migrate because the exposed side of the island is constantly eroded by wave action. These islands lack healthy dune systems and backshore vegetation that act as sand anchors on the beach. This deficiency makes the islands susceptible to erosion, allowing wind-generated waves to carry sediment from the beaches to the backside of the island by over-washing processes. Due to the flooding of storm waves over the island, dead mangroves of *Rhizophora* and *Avicennia* as well as peat soils of former backside mangrove swamps are exposed on the shoreline (Fig. 7E–H).

Erosion of mangroves is a common geomorphic feature in the Patía southern delta lobe (Fig. 8J–K). This former delta plain, exposed to predominant wind waves from the southwest, lacks sufficient sediment for the offshore zone to build shoals, which could mitigate the effects of wave action and sea-level rise. Some barrier islands, including those at Pasacaballos and San Juan de la Costa (Fig. 8I), have retreated as much as 500 m after the occurrence of both events, the 1979 tsunami and the more pronounced flow diversion during the 1980s.

4.4. Coastal erosion and accretion rates 1986–2008

Rates of shoreline change were calculated at each transect using the statistical technique of End Point Rate (EPR) applied to all four shoreline positions from the earliest in 1986 to the most recent in 2008 (Fig. 8). For the southern Patía Delta front, between locations E and H (Fig. 8), the percentages of coastline experiencing erosion, averaged over 602 transects, were 60% and 56% for the 1986–2001 and 2001–2008 periods, respectively. Higher coastal land losses of 104 and 39 m for the period 1986–2001 were observed at Pasacaballos (Fig. 8E) and Patía (Fig. 8H) inlets, respectively. Overall, the southern delta lobe experienced an average erosion rate of -2.31 m/yr (-16.2 m average retreat) during the period 2001–2008. It is worth noting that for the same time period, accretion processes only occurred along 4% of the coast in this region.

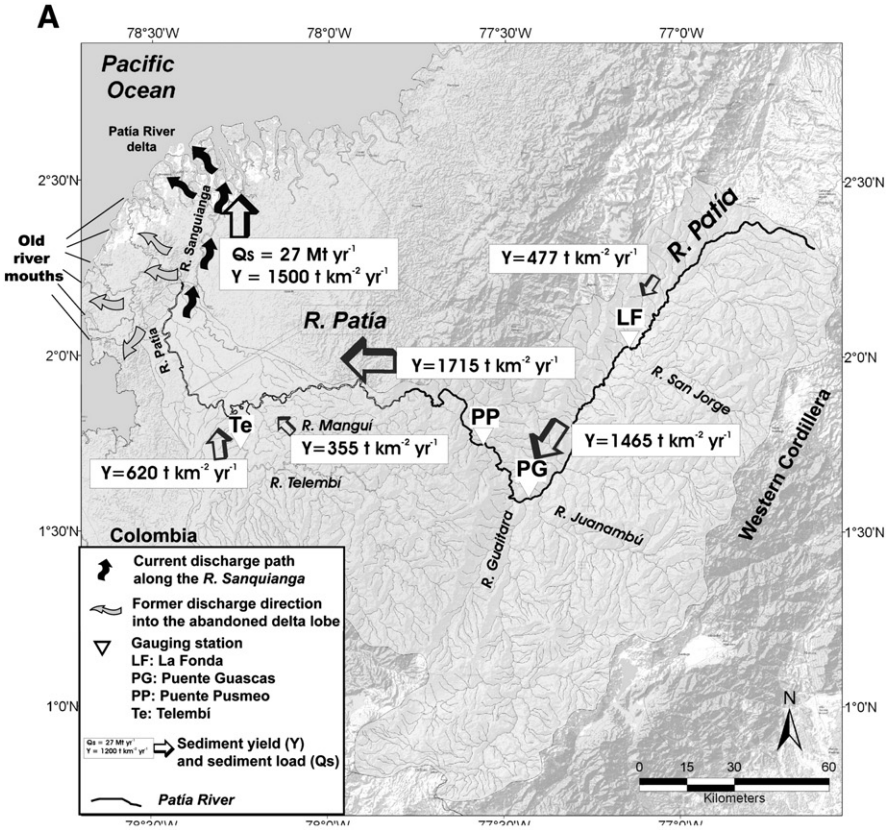
A
78°30'W
78°0'W
77°30'W
77°0'W
Pacific Ocean
Patia River delta
2°30'N
2°0'N
1°30'N
1°0'N
Old river mouths
R. Sanquianga
R. Patía
Qs = 27 Mt yr-1
Y = 1500 t km-2 yr-1
Y=477 t km-2 yr-1
R. Patía
LF
Y=1715 t km-2 yr-1
R. San Jorge
Western Cordillera
PP
Te
R. Manguí
Y=355 t km-2 yr-1
Y=1465 t km-2 yr-1
PG
Y=620 t km-2 yr-1
R. Telembí
R. Juanambú
R. Guaitara
Colombia
Current discharge path along the R. Sanquianga
Former discharge direction into the abandoned delta lobe
Gauging station
LF: La Fonda
PG: Puente Guascas
PP: Puente Pusmeo
Te: Telembí
Sediment yield (Y) and sediment load (Qs)
Patía River
N
0 15 30 60
Kilometers

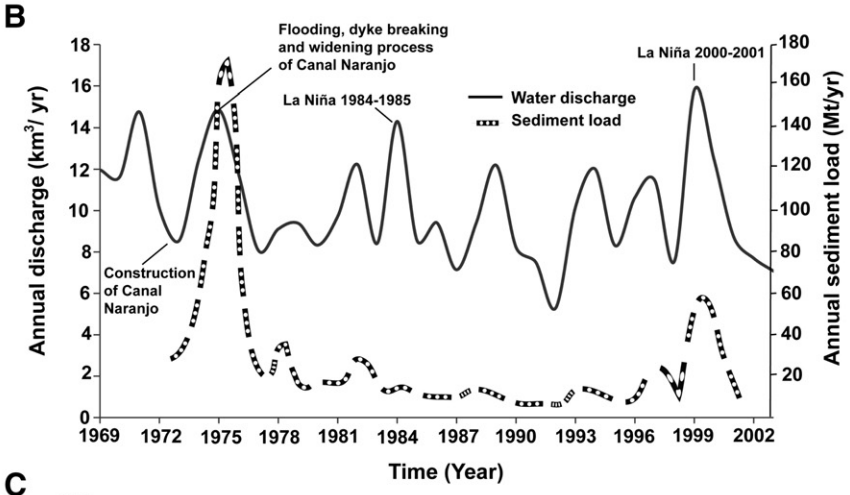
B
Flooding, dyke breaking and widening process of Canal Naranjo
La Niña 1984-1985
La Niña 2000-2001
Water discharge
Sediment load
Annual discharge (km3/ yr)
Annual sediment load (Mt/yr)
Construction of Canal Naranjo
Time (Year)

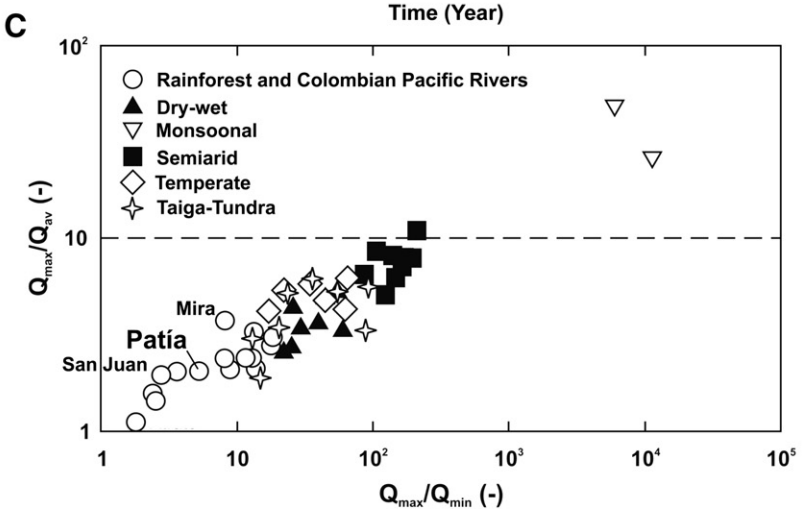
C
Rainforest and Colombian Pacific Rivers
Dry-wet
Monsoonal
Semiarid
Temperate
Taiga-Tundra
Qmax/Qav (-)
Mira
Patía
San Juan
Qmax/Qmin (-)

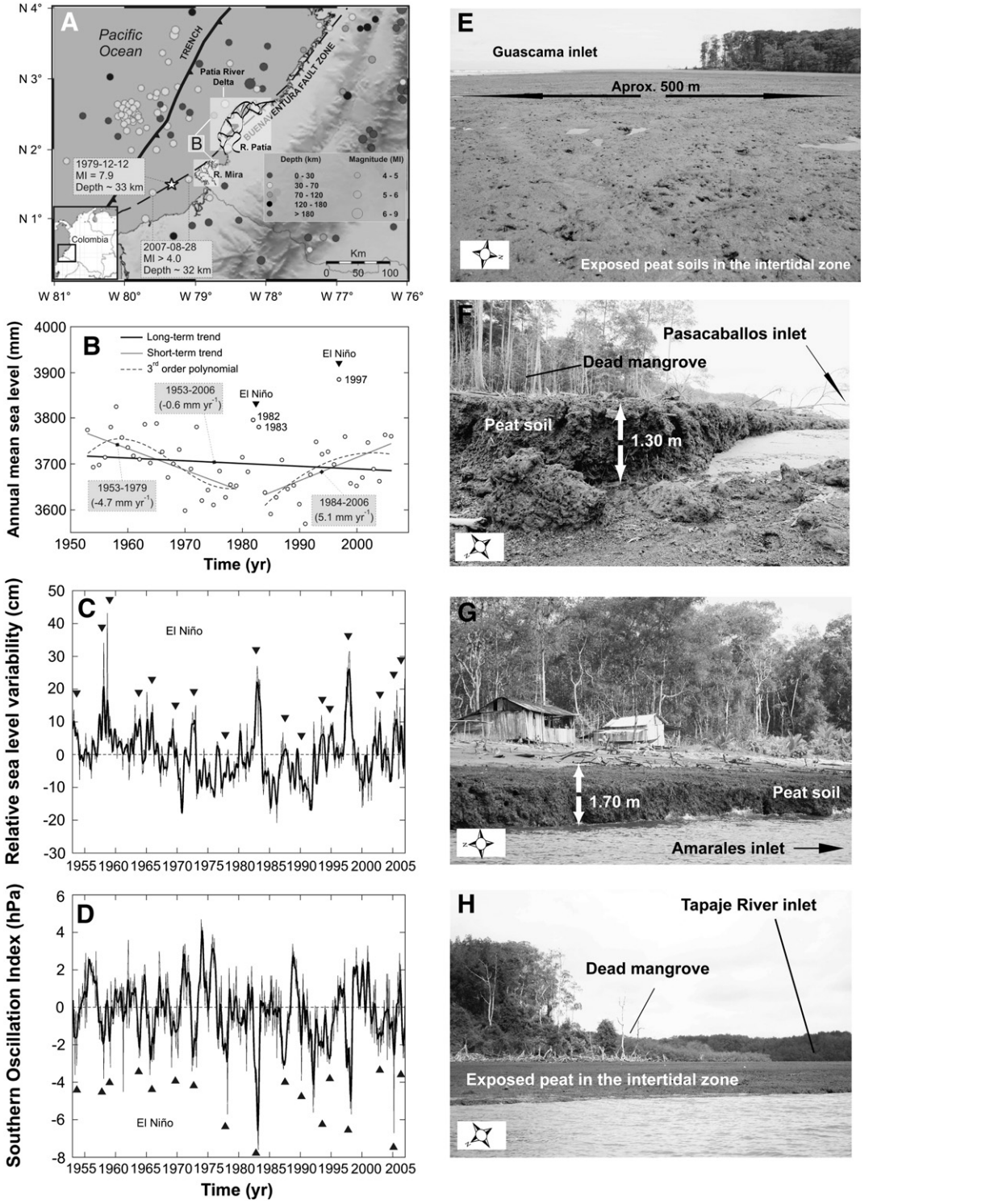

Fig. 7. (A) Location and magnitude of earthquakes that occurred in the southern Colombian Pacific between 1993 and 2007. More than 120 seismic events with magnitudes (MI) greater than 4, were recorded by the Geological Survey of Colombia between 1993 and 2007 (INGEOMINAS, 2007). Also shown are the locations of two recent seismic events (August 2007) and the tsunami (December 1979) (white star) that impacted the Patía delta coast. (B) Mean relative sea-level (mm) from Tumaco, Pacific coast of Colombia (IDEAM, 2007), showing the trend for the 1953–2006 period with slope = -0.6 mm yr^{-1} (bold line) and the short-term trends (grey line) for the 1953–1979 period (slope = -4.7 mm yr^{-1}) and 1984–2006 period (slope = 5.1 mm yr^{-1}). Solid triangles indicate the occurrence of two major El Niño sea-level anomalies in 1982–1983 and 1997, which were removed from the analysis (after López et al., 2009). (C) Monthly average (thin line) and low-frequency pass filter with zero-phase (bold line) plots of water-level anomalies at Tumaco in 1953–2006. (D) The atmospheric pressure difference (millibar) at sea level between Darwin, Australia, and Tahiti. The SOI is negative during El Niño years and positive during La Niña years. The SOI data were obtained from the NOAA database. We also show the exposed peat soils on the beach along barrier islands in the Guascama (E), Pasacaballos (F), Amarales (G) and Tapaje (H) inlets. Note strong conditions of mangrove erosion on the shoreline.

Fig. 6. (A) Map of the Patía River drainage basin, showing the principal tributaries, the four hydrological stations (triangles) where water discharge and sediment load are gauged, and the mean annual sediment load values at the upper, middle and lower reaches of the Patía River (arrows). (B) Plots of river discharge data for the 1967–2002 year-period and annual sediment load for the 1972–2001 year-period (dotted line) of the Patía River as gauged at Puente Pusmeo. (C) Discharge variability for world tropical rivers in different hydrologic and morphoclimatic zones. Colombian rivers show the lowest values of Q_{max}/Q_{mean} and Q_{max}/Q_{min} ratios compared to other rainforest rivers (modified from Latrubesse et al., 2005).

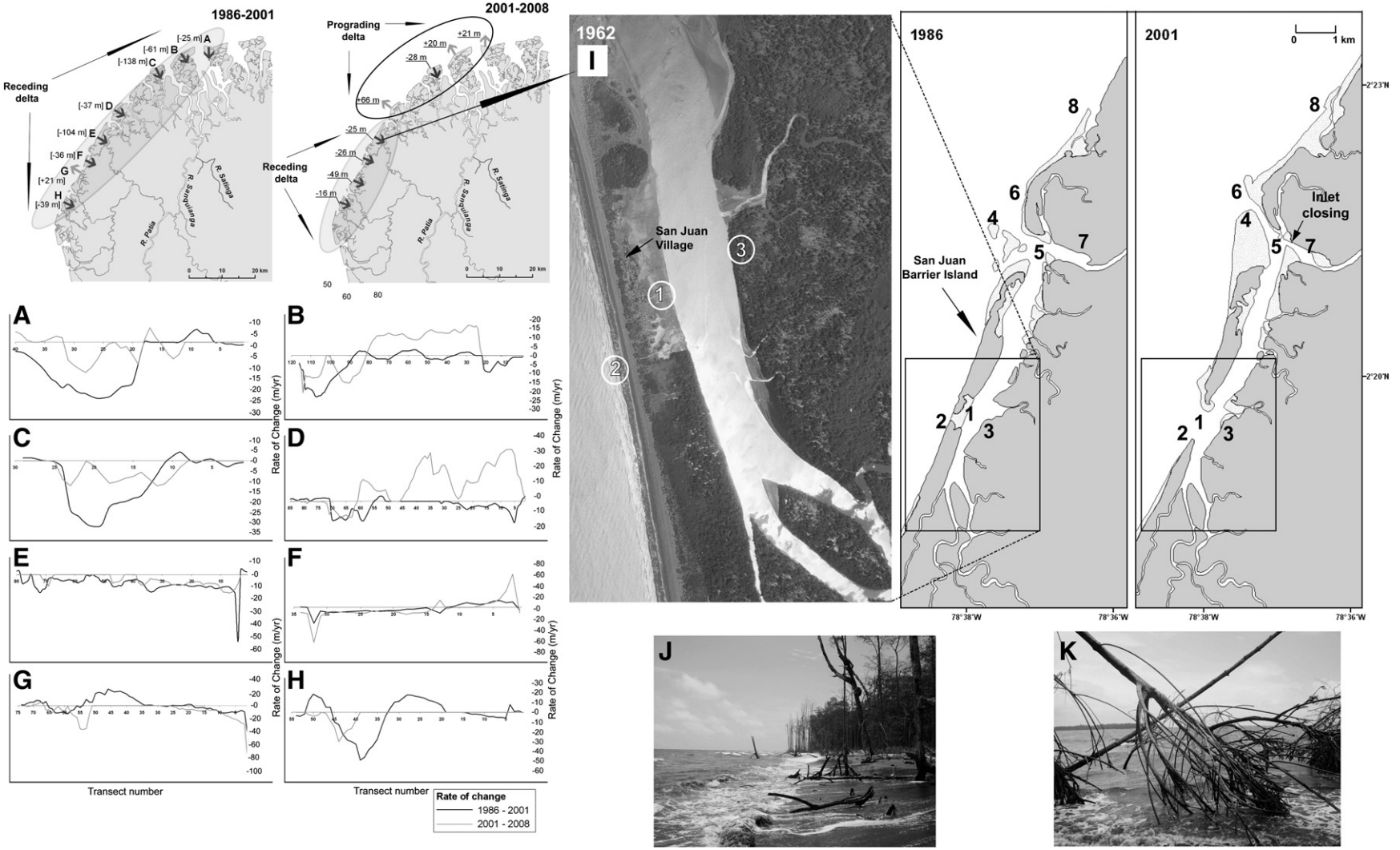

Fig. 8. (A–H) Shoreline positions of the analyzed areas that are generated from the satellite data and DSAS software for the 1986–2001 and 2001–2008 periods. The estimated rates of shoreline changes (erosion or accretion) calculated at each transect are plotted alongshore in each coastal site. The location of each shoreline segment and the corresponding coastal land loss are shown in the maps (top).(I) Temporal analysis of morphological changes along the San Juan barrier island, southern delta coast, based on aerial photographs from 1962 and Landsat images from 1986 to 2001.(J–K) Marked mangrove erosion on the southern delta shoreline.

Along the northern delta front, between locations A and D (Fig. 8), erosion conditions for the 1986–2001 and 2001–2008 periods were observed in 69% and 22% of the analyzed shoreline transects, respectively. Major retreating zones during the period 1986–2001 include Sanquianga (B), Guascama (C) and Chitaco (D) barrier islands, with average coastal land losses of 61, 138, and 37 m, respectively. An erosional coastline with weak beach development, dead mangrove, and exposed peat soils in the surf zone characterized the entire area.

In general, the whole delta front experienced retreat conditions during the period 1986–2001. However, the northern delta region (Fig. 8A–D) showed signs of accretion during the period 2001–2008. The discharge diversion of the Patía River to the Sanquianga has apparently balanced the observed trends in coastal erosion and sea-level rise along the active delta lobe in the Sanquianga area. However, overall coastal retreat was still evident along the southern delta lobe and the system has still not reached an equilibrium phase (Fig. 8D–H).

Further analysis of coastal geomorphology in the southern delta lobe between 1962 and 2001 indicates major morphological changes during the 39-year period, including: (1) strong retreating conditions at the San Juan barrier island (Fig. 8I); landward erosion resulted in a breaching event after the occurrence of the 1979 tsunami; (2) abandonment of active distributary channels as a result of the flow diversion from the Patía to the Sanquianga River; (3) closing of active distributary inlets at Majagual, Patía, and Salahonda (Fig. 1B); and (4) formation of ebb tidal deltas at the distributary mouths (Fig. 8I).

4.5. Geomorphic changes in the Sanquianga mangrove reserve, northern Patía delta

The migration of the active distributary channel from the southern lobe to the northern delta plain has led to active sedimentation, overbank flow, increasing width of levees, sedimentation in crevasses, interdistributary channel fill (Fig. 9), and further lengthening of the Sanquianga River, the current main distributary channel.

There have been inferred from the present mangrove distribution in the Sanquianga River several stages in the process of channel lengthening and the corresponding sequence of vegetation change (Fig. 9). (A) During the seaward advance of the Sanquianga distributary channel, submerged levees gradually emerged above sea level due to active sedimentation of fine sediment deposited by overbank flow. (B) Pioneer mangroves started to colonize the fine sediments of levees and mudflats, particularly those areas which were exposed during low tide conditions. Once the levee height above low water level reached its maximum, the process of channel fill in the interdistributary channel began. (C) Once the interdistributary channel fill was completed, pioneer mangroves colonized the lateral channel. (D) Stages A, B, and C continued progressively downstream and the banks of the Sanquianga River show the sequence of longitudinal advance, as seen by the periodic lows and highs of mangrove heights along the channel (Fig. 9D).

Temporal analysis of morphological changes at the current delta apex, Bocas de Satinga, based on aerial photographs from 1962 and an Aster image from 2008 (Fig. 9E–F), shows major areas of sedimentation and channel fills in the Sanquianga distributary channel and associated tidal creeks during the 46 yr-period. This process of distributary channel advance was actively initiated after the diversion event started 37 years ago. According to local inhabitants, the colonization and further growth of these mangrove communities took place in approximately 30 years and sedimentation from the delta apex at Bocas de Satinga to the Sanquianga River have become more pronounced since the 1990s (Fig. 5). Although the conditions of channel diversion shifted the sedimentation from the Patía River to the Sanquianga, giving the constructive conditions for mangrove colonization, the increased water discharge has freshened the former estuarine system and created different hydrologic conditions with further ecological implications.

Longitudinal measurements of vertical profiles of salinity (psu) along the main axis of distributary channels, including Sanquianga, Guascama and Amarales (Fig. 1B), show clear dependence on the discharge pattern of the deltaic plain. Prior to the channel diversion, the 1 psu salinity interface at the bottom intruded 25 km further upstream up to Bocas de Satinga, the current delta apex. Nowadays the 0 psu salinity interface near the bottom is found 13, 15 and 32 km upstream on the Sanquianga, Guascama, and Amarales distributaries, respectively (Fig. 10A). The longitudinal salinity distribution qualitatively reflects the amount of freshwater discharged by the Sanguinga River. Also, the effect of increased freshwater after the channel diversion is to flush out the wedges of saline waters from the main distributary channels. In contrast, abandoned distributaries of the former Patía delta (e.g., Pasacaballos inlet) (Fig. 1B), which currently lack fluvial flows for at least 8 months each year, possess more saline waters and exhibit increased salinity distributions further upstream.

In particular, the Sanquianga and Guascama distributaries are influenced by increased fluvial discharge and their former limits of saline intrusion have been shifted downstream. On the contrary, the Amarales channel has seen its saline wedge moved further upstream, possibly indicating increased salinity intrusion (Fig. 10A). Major environmental consequences of the Patía River discharge diversion, in terms of geomorphic impacts on mangrove ecosystems, are evidenced by freshening conditions in the Sanquianga and Guascama distributary channels, a hydrologic change that has allowed the downstream advance of freshwater vegetation, which is invading channel banks in the lower and mixing estuarine zones.

The analysis of vegetation cover of selected locations in the Sanquianga mangrove reserve from 1986 to 2001, prepared from the classification of MSS and TM Landsat images (Fig. 10B–D), shows that at the current delta apex, mixed and freshwater vegetation increased its area during the 15-year period (Fig. 10D); an increase mainly attributed to the freshening conditions and clearing of forest. In fact, mixed vegetation cover increased its area by 970 ha during the analyzed time period. Dense mangrove forests were estimated to have declined from 1012 ha in 1986 to 660 ha in 2001. Also, low dense mangrove cover decreased by approximately 500 ha during the same time period. Thus, it seems reasonable to propose that the remarkable increase in water discharge is expected to show shifting conditions in the patterns of vegetation succession. Downstream along the Sanquianga distributary channel, the images also indicate that dense mangrove cover increased by 1000 ha (Fig. 10B); an increase accounted for by the above-mentioned process of channel lengthening and the corresponding sequence of vegetation change. In contrast to the observed vegetation changes along the active distributaries, mangrove cover along the Amarales branch, an estuarine channel with no fluvial discharge, remain approximately constant for the analyzed time period (Fig. 10C).

4.6. Wave conditions and their implications for shoreline dynamics

The NWW3 wave data indicate that the observed waves in the Patía delta are predominantly swells from the southwest (77%) with a maximum monthly significant height of 2.2 m, and an average peak period of 14 s (Fig. 11C). Also, the AWAC time series measurements of wave parameters at five stations in the Patía delta front show that waves at the 10 m isobath have significant wave heights ranging from 0.54 to 1.4 m and a mean peak period of 14 ± 0.7 s. The wave power climate can be expressed by combining the effects of all datasets of wave characteristics for each month. This is done by taking the monthly weighed means of the total and longshore power values. The analysis of total wave power per unit crest width along the delta front indicates that the Patía delta exhibits moderate

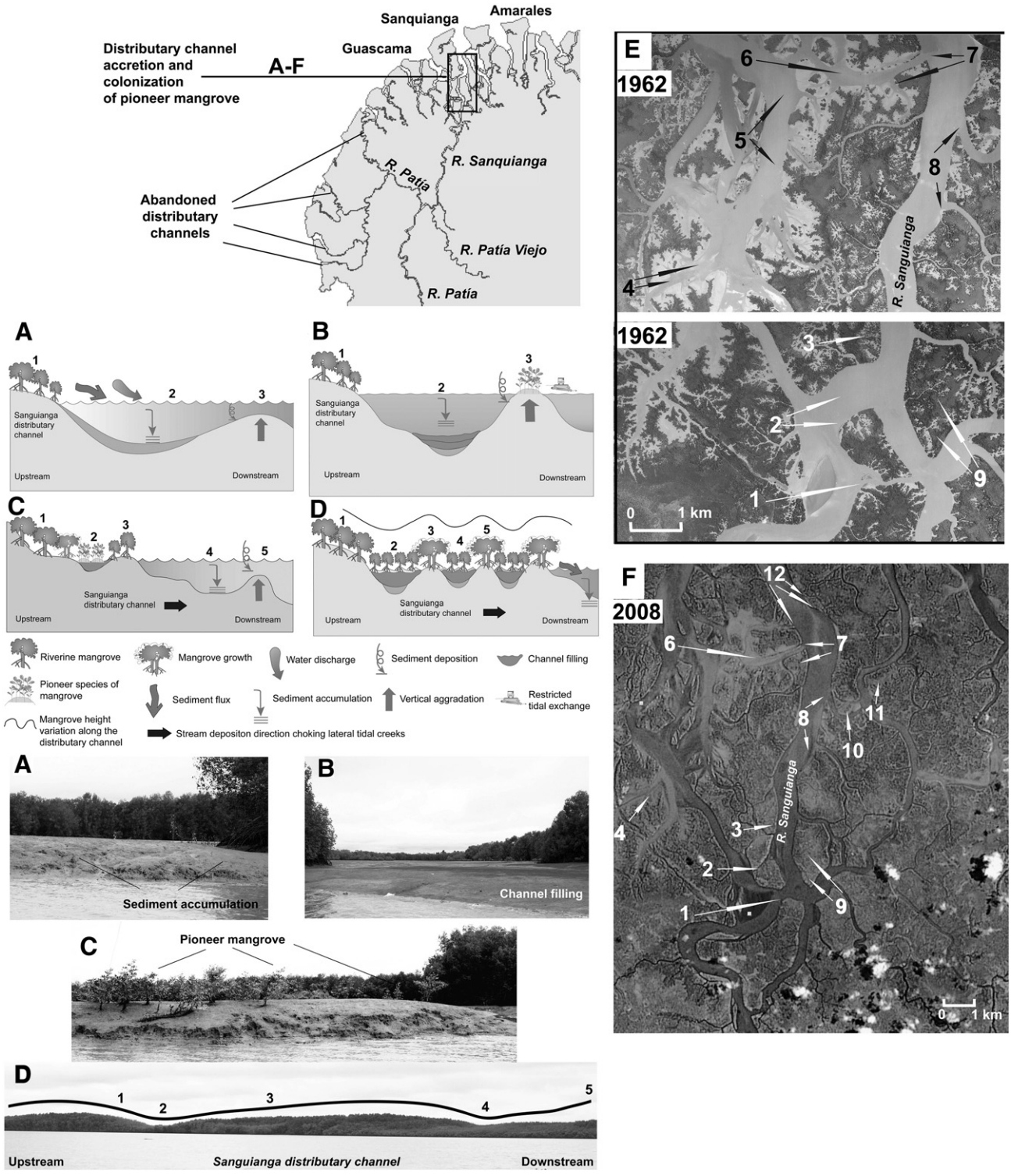

Fig. 9. (A–D) Stages of channel lengthening and corresponding sequences of mangrove colonization along the Sanquianga distributary channel. (E–F) Temporal analysis of morphological changes at the current delta apex, Bocas de Satinga, based on (E) aerial photographs from 1962 and (F) Aster image from 2008. Numbers indicate major areas of sedimentation and channel fills in the Sanquianga distributary channel and associated tidal creeks.

wave energy conditions with an average wave power of ~18×10^6 erg s^{-1} m at the 9 m depth contour.

Observations along the sub-aqueous deltas of major rivers, including the Amazon (Nittrouer et al., 1996), the Mahakam (Storms et al., 2005), the Ganges–Brahmaputra (Kuehl et al., 1997), the Po (Cattaneo et al., 2003), and the Fly (Harris et al., 2004), suggest that the depositional mechanisms of sub-aqueous deltas are controlled by energetic marine environments, which are related to energetic waves and meso- to

Fig. 10. (A) Vegetation cover image of the northern Patía–Sanquianga delta lobe, based on the classification of a TM Landsat image 2001. Major longitudinal limits of salinity intrusion and downstream limits of freshwater vegetation are also shown. (B–D) Vegetation cover analysis of selected locations in the Sanquianga mangrove reserve from 1986 to 2001 prepared from the classification of MSS and TM Landsat images, showing major cover changes in the Sanquianga (B), Amarales (C), and Bocas de Satinga areas (D).

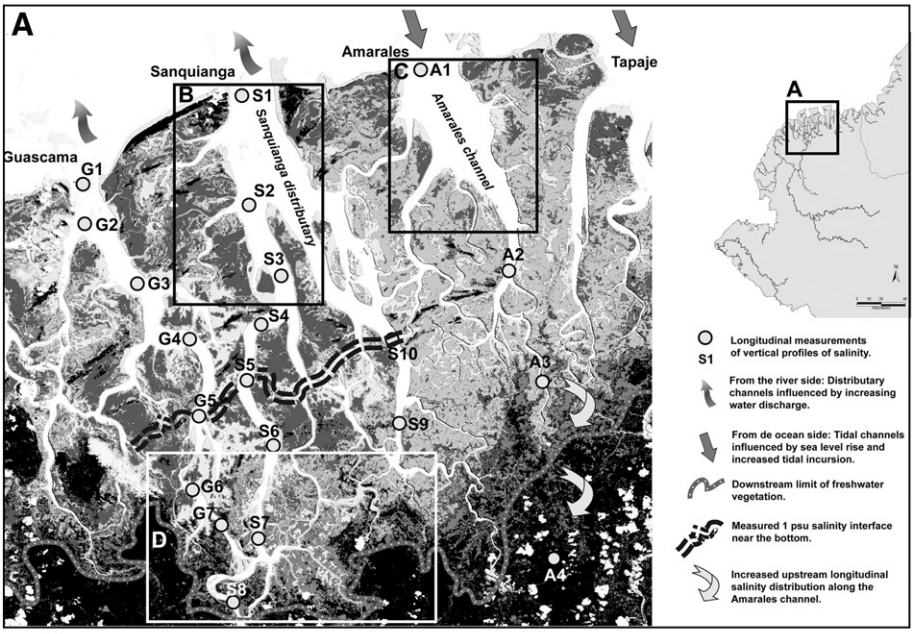
A
Sanquianga
Amarales
Tapaje
Guascama
B
C
D
S1
A1
G1
S2
G2
S3
A2
G3
S4
G4
S10
S5
A3
G5
S9
S6
G6
G7
S7
S8
A4
Sanquianga distributary
Amarales channel
Longitudinal measurements of vertical profiles of salinity.
From the river side: Distributary channels influenced by increasing water discharge.
From de ocean side: Tidal channels influenced by sea level rise and increased tidal incursion.
Downstream limit of freshwater vegetation.
Measured 1 psu salinity interface near the bottom.
Increased upstream longitudinal salinity distribution along the Amarales channel.

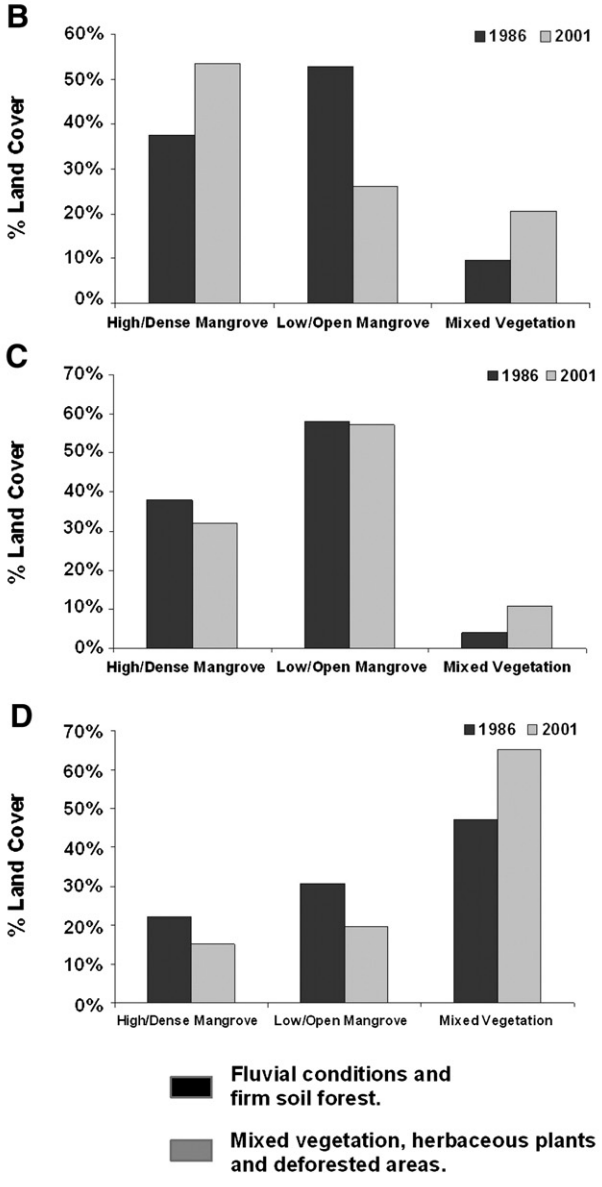
B
C
D
% Land Cover
1986
2001
High/Dense Mangrove
Low/Open Mangrove
Mixed Vegetation
Fluvial conditions and firm soil forest.
Mixed vegetation, herbaceous plants and deforested areas.

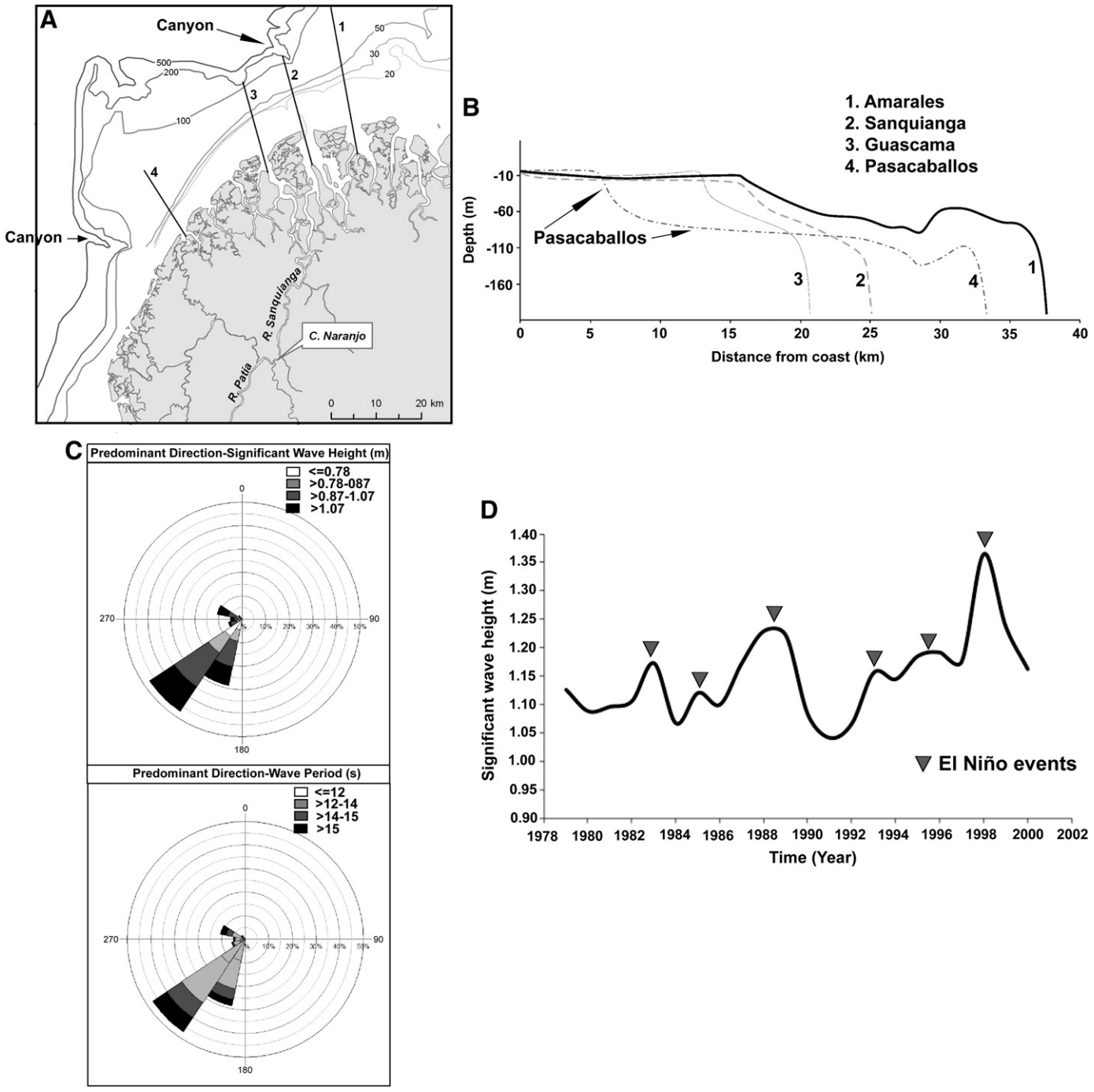

Fig. 11. (A) Map of the Patía delta showing major isobaths and locations of bathymetric profiles along the delta front. (B) Bathymetric profiles of subaqueous sections based on bathymetric maps from the hydrographic service of the Colombian Navy (unpublished data). (C) Predominant wave direction diagrams for the Patía River delta, showing magnitudes of significant wave height and wave period. (D) Plot of annual means of significant wave height (H_s) at the Patía delta front derived from the NWW3 wave data 1979–2000.

macro-tidal ranges. Each sub-aqueous delta is different in size and morphology due to differences in fluvial discharge, shelf bathymetry, and the local oceanographic regime (Storms et al., 2005). For the Patía Delta, the shape of sub-aqueous profiles may be entirely flat (Guascama and Sanquianga inlets) and angular-shaped (Pasacaballos inlet in the southern delta plain) (Fig. 11). The 10-m isobath extends 16, 14, and 6 km offshore in the Sanquianga, Guascama, and Pasacaballos inlets, respectively (Fig. 11B). Probably, the deeper depths of the delta-front platform of the Pasacaballos inlet may be attributed to the high and moderate wave energy on the southern delta coast.

The degree to which wave power is reduced by the offshore slope is indexed by an attenuation ratio (A_p). This index, developed by Bretschneider (1954) and Bretschneider and Reid (1954), estimates the reduction of wave height due to bottom friction (Wright and Coleman, 1973). In the Patía Delta, the attenuation ratios indicate that friction reduces nearshore power to 16% of the deep-water power in the Pasacaballos inlet, while in the Guascama and Sanquianga inlets, the A_p values are higher and wave power is reduced by 67% and 82%, respectively. The steeper profile in the southern delta plain at Pasacaballos causes less reduction of wave power due to friction. This morphologic condition may be responsible for the lowest attenuation ratio along

the Patía delta front, and hence ongoing erosional conditions at Pascaballos. Based on the NWW3 wave data 1979–2000, annual means of significant wave height (H_s) at the Patía Delta front, are shown in Fig. 11D.

Overall, there is a good agreement between sea-level anomalies during El Niño events and significant wave heights. During El Niño periods in 1982–1983, 1987–1988, 1992–1993, and 1997–1998, H_s were considerably higher than the interannual mean of 0.93 m. In general, wave heights during raised sea-level conditions are higher than the inter-annual mean by 30%, indicating increasing wave energy conditions at the Patía Delta coast.

5. Discussion

5.1. Effects of tectonic activity on delta migration and channel diversion

As mentioned before, the overall southward displacement of the main distributary channels in the San Juan and Patía deltas has been associated with the presence of active transcurrent and transverse fault systems (Fig. 2A–B) (Gómez, 1986a, 1986b; Correa, 1996; González et al., 2002 and Restrepo et al., 2002). In the Mira River delta (Fig. 2C), evidence of paleochannels also suggests that delta distributaries have undergone rearrangements due to seismic movements registered since 1906 (Gómez, 1986a). Transcurrrent faulting associated with several transverse paleofracture zones, including the Tumaco fault and the Mira River alignment, may have influenced the discharge displacement from the northern distributary emptying into Bocagrande, a distributary inlet present in 1783, to the Mira River distributary and its current location at Milagros Frontera. Thus, the Holocene evolution of the Colombian Pacific deltas, including the Patía, has been characterized by a spatial switch of delta distributaries related to tectonic movements and subsidence.

Tectonic activity in the Patía River's drainage basin along an active fault increased the discharge diversion of the Patía River even more as a result of the 1979 earthquake. Due to the 1979 seismic event, there was an uplift movement that resulted in the Sanquianga River capturing approximately 70% of the Patía River's discharge (Soeters and Gómez, 1985; Velásquez et al., 1994). An analysis of cross-profiles at the confluence of the Patia and the Sanquianga rivers based on space shuttle radar topography mission (SRTM) elevation data obtained at 2002, which has a ~90 m horizontal and a 1 m vertical resolution (Restrepo and Kettner, 2012), indicates that the land and freshwater surface of the partly abandoned Patia River are located slightly higher (7 m) than the Sanguianga cross-profiles, indicating that the hydraulic capacity of the Sanquianga is even more pronounced. Based on water discharge measurements in 1987 (Velásquez et al., 1994), more than 80% of the Patía River discharge was redirected through the Canal Naranjo – Patía Viejo distributary – to the Sanquianga River system (Fig. 5). Presently, the Sanquianga River, discharging into Bocas de Satinga to the north (Fig. 1B), now carries more than 90% of the Patía riverine flux (Bateman et al., 2009).

5.2. Eustatic and relative sea-level change

The 1982 El Niño in the eastern equatorial Pacific was remarkable. By October, SST was almost 5 °C above normal and the sea level at the Galapagos Islands had risen by 22 cm (Cane, 1983). Also, during the 1998 El Niño, equatorial waters in the eastern Pacific were 3–4 °C warmer and 20–30 cm higher than normal (Morton et al., 2000). In Tumaco, strong El Niños in 1982 and 1998 raised sea levels by 28 cm and 32 cm, respectively. Moderate El Niño events in 1958, 1965, 1969, 1972, 1987, and 1992 raised the water level by 10–44 cm along the Patía delta (Fig. 7C).

Ongoing tectonically-driven subsidence of the entire delta plain is an important factor in the fluvial sediment supply to the islands. Channel switching deprives the delta of sediment as the abandoned areas subside, the older distributary mouths become flooded or drowned. This may be the former case of the northern Patía–Sanquianga River delta before the channel diversion occurred. In contrast, current conditions are characterized by active sedimentation at the delta apex, downstream channel accretion and sediment deposition in estuarine lagoons. Although the northern delta lobe shows signs of coastal subsidence along transgressive barrier islands, our analysis of satellite images during low tide conditions for the period 1986–2001 in the Sanquianga inlet, indicates an increase in tidal flat area from 5.4 M m^2 in 1986 to 14 M m^2 in 2001. In addition, the analysis of shoreline change for the period 2001–2008 shows signs of accretion (Fig. 8). Hence, the Sanquianga River, a distributary channel experiencing an accretional phase, is switching from previous estuarine conditions to an active delta system.

According to interviews with the local inhabitants in Mulatos village (Sanquianga inlet), the occurrence of non-storm washover of barrier islands was not linked with raised sea levels due to ENSO events prior to the tsunami in 1979. However, the El Niño events in 1982–1983 and 1997 created non-storm overwash on the barrier islands at Pasacaballos, San Juan de la Costa and Salahonda (Fig. 1B) and eroding conditions started to prevail 25 years ago, just after the El Niño 1982–1983 event (Fig. 8). The agreement of relative sea-level changes for the 1979–2006 year period with tectonic setting (Figs. 1 and 7), and the occurrence of non-storm washover events and earthquake activity may suggest that subsidence is continuing in the southern delta lobe. Thus, the recent evolution of the Patía delta has been characterized by short-term constructive and destructive phases due to the interaction between tectonically- and eustatically-induced sea-level rises and fluvial fluxes.

5.3. Salinity distribution and associated vegetation changes

Inundation frequency and longitudinal salinity distribution have major effects on mangrove distribution. Saline intrusion varies primarily with freshwater discharge, which controls inundation, substrate composition, and distribution of fringing vegetation within the distributary channel network in tropical deltas (Vann, 1959; Thom, 1967; Restrepo and Kjerfve, 2002). Freshening conditions in the Sanquianga distributary channel have shifted the upper estuarine region downstream (salinity<1 psu) (Fig. 10A). According to local inhabitants in the area (from personal communication with Wilfrido Ibarbo), the effect of increased freshwater discharge on plant ecology has become more pronounced during the last decade. Near the current delta apex at Bocas de Satinga, characteristic grasses of fluvial environments such as *Panicum* and *Paspalum*, are colonizing point bars and mudflats in front of the channel banks which are vegetated by *Rhizophora*. In addition, the locally called Nato (*Mora oleifera*), a mangrove tolerant of brackish water and also characteristic of the freshwater swamp zone, are invading channel banks in the lower and estuarine mixing zones.

The above-mentioned changes observed in the mangroves of the SMNP are primarily the response to an ever-changing series of habitats, the result of geomorphic changes associated with the development of an active delta plain. Similar processes have been observed in other deltas, including Tabasco, Mexico (Thom, 1967), Mira and San Juan, on the Pacific coast (West, 1957; Restrepo et al., 2002), Atrato, on the Caribbean coast of Colombia (Vann, 1959), and are similar to the Purari, Papua New Guinea (Conn, 1983). The observed geomorphic changes in the northern lobe of the Patía delta are the first environmental signs of shifting conditions from an estuary to a delta system as these processes act on long-term timescales.

6. Conclusions

The recent evolution of the Patía delta has been controlled by the interplay of extreme hydrologic, geologic, oceanographic and

anthropogenic conditions, including: (1) highest basin-wide sediment load of any river on the west coast of South America; (2) low discharge variability (Q_{max}/Q_{min}); (3) tectonic depression associated with faults and the occurrence of large magnitude, shallow focus earthquakes; (4) spatial switch of delta distributaries related to tectonic movements and subsidence; (5) a relative sea-level rise of 5.1 mm yr^{-1} after the occurrence of the 1979 tsunami; (6) strong oceanographic manifestations associated with the ENSO cycle, causing sea-level rises of 10–44 cm during El Niño years; and (7) human-induced discharge diversion that shifted the active delta plain back to the its former location and changed the northern estuarine system into an active delta plain.

The Patía delta provides a unique example of one of the few deltas worldwide formed under the occurrence of highly energetic and destructive environmental conditions. The data and analysis presented here provide key information towards addressing important issues in terms of global delta dynamics and vulnerability, including those posed by Overeem and Syvitski (2009): (1) delta progradation and the receding conditions; (2) catchment and basinal processes influencing delta form; (3) environmental stresses on deltas (physical and social); and (4) the role of extreme events versus 'normal' conditions in creating and shaping deltas.

Acknowledgements

This study was supported by the Instituto Nacional para el Desarrollo de la Ciencia y la Tecnología "Francisco José de Caldas", COLCIENCIAS, grant 1216-452-21267 (Morphodynamics of the Patía River delta, Pacific coast of Colombia), EAFIT University—Department of Geological Sciences, and the Colombian Port Authority, DIMAR, through its research institute CCCP (Centro de Investigaciones Oceanográficas del Pacífico) in Tumaco, Colombia. Special thanks to the reviewers and the editor for their constructive comments and corrections, which have improved the manuscript considerably. The revised version of this paper was done during a Tinker Visiting Professorship at the Teresa Lozano Long Institute of Latin American Studies, University of Texas at Austin.

References

Bateman, A., Medina, V., Coliles, A., Loaiza, A., García, W., Puig, C., 2009. The impressive case of the uncontrolled diversion of the Patía River at its delta and the social and environmental consequences. Proceedings of the Congress of River, Coastal and Estuarine Morphodynamics (RCEM, 2009). Universidad Nacional del Litoral, Santa Fe, Argentina.

Bretschneider, C.L., 1954. Field investigation of wave energy loss in shallow water ocean waves. US Army Corps Engineers Beach Erosion Board Tech. Special Publication, 46, pp. 1–21.

Bretschneider, C.L., Reid, O., 1954. Modification of wave height due to bottom friction, percolation and refraction. US Army Corps Engineers Beach Erosion Board Tech. Special Publication, 45. 36 pp.

Cane, M.A., 1983. Oceanographic events during El Niño. Science 222, 1189–1210.

Cattaneo, A., Correggiari, A., Langone, L., Trincardi, F., 2003. The late-Holocene Gargano subaqueous delta, Adriatic shelf: sediment pathways and supply fluctuations. Marine Geology 193, 61–91.

Conn, B.J., 1983. Aquatic and semi-aquatic flora of the Purari River system. In: Petr, T. (Ed.), The Purari-Tropical Environment of a High Rainfall River Basin. Dr. W. Junk Publishers, The Hague, The Netherlands, pp. 283–293.

Correa, I.D., 1996. Le littoral Pacifique Colombien: interdependance des agents morphostructuraux et hydrodynamiques - Tome 1: texte. Ph.D. dissertation, Universite Bordeaux I, Bordeaux, France, 178 pp.

Correa, I.D., González, J.L., 2000. Coastal erosion and village relocation: a Colombian case study. Ocean and Coastal Management 43, 51–64.

Enfield, D.B., Allen, J.S., 1980. On the structure and dynamics of monthly mean sea levels anomalies along the Pacific coast of North and South America. Journal of Physical Oceanography 10, 557–578.

Ericson, J.P., Vörösmarty, C.J., Dingman, S.L., Ward, L.G., Meybeck, M., 2006. Effective sea-level rise and deltas: causes of change and human dimension implications. Global and Planetary Change 50, 63–82.

Gómez, H., 1986a. Contribución geomorfológica y estructural del suroccidente colombiano y de la costa pacífica entre Tumaco-Buenaventura y Quibdo. CIAF, Bogotá. 33 pp.

Gómez, H., 1986b. Algunos aspectos neotectónicos hacia el suroeste del Litoral Pacífico colombiano. Revista CIAF 11, 281–289.

González, J.L., Correa, I.D., Aristizábal, O., 2002. Evidencias de subsidencia cosísmica en el delta del San Juan. In: Correa, I.D., Restrepo, J.D. (Eds.), Geología y oceanografía del delta del río San Juan: litoral Pacífico colombiano. Fondo Editorial Universidad EAFIT, Medellín, pp. 89–110.

Harris, P.T., Hughes, M.G., Baker, E.K., Dalrymple, R.W., Keene, J.B., 2004. Sediment transport in distributary channels and its export to the pro-deltaic environment in a tidally dominated delta: Fly River, Papua New Guinea. Continental Shelf Research 24, 2431–2454.

Herd, D.G., Youd, T.L., Meyer, H., Arango, J.L., Person, W.J., Mendoza, C., 1992. The great Tumaco, Colombia earthquake of December 1979. Science 211, 441–445.

Hori, K., Saito, Y., 2007. Classification, architecture and evolution of large river deltas. In: Gupta, A. (Ed.), Large Rivers: Geomorphology and Management. John Willey and Sons, New York, pp. 75–96.

IDEAM, 2007. Datos Horarios del nivel relativo del mar para la estación mareográfica de Tumaco, 1953–2006. Instituto de Hidrología, Meteorología y Estudios Ambientales IDEAM. Digital format.

IDEAM, 2009. (Data). River database of the Patía drainage basin. Instituto de Hidrología, Metereología y Estudios Ambientales (IDEAM), Bogotá, Colombia (5 gauging stations). .

INGEOMINAS, 2007. Sismicidad registrada por la Red Sismológica Nacional de Colombia (Junio de 1993 a Septiembre de 2007). Mapa del Pacífico sur colombiano, Ingeominas, Bogotá.

Kellogg, J.N., Mohriak, W.U., 2001. The tectonic and geological environment of coastal South America. In: Seeliger, U., Kjerfve, B. (Eds.), Coastal Marine Ecosystems of Latin America. Springer Verlag, Berlin-Heilderberg, pp. 2–16.

Kuehl, S.A., Levy, B.M., Moore, W.S., Allison, M.A., 1997. Subaqueous of the Ganges–Brahmaputra river system. Marine Geology 144, 81–96.

Latrubesse, E.M., Stevaux, J.C., Sinha, R., 2005. Tropical rivers. Geomorphology 70, 187–206.

Lockridge, P.A., Smith, R.H., 1984. Tsunamis in the Pacific Basin 1900–1983: Map (1:17,000.000). National Geophysical Data Center, Boulder, Colorado.

López, S.A., Restrepo, J.D., Restrepo, J.C., Monroy, C., Mora, H., Rubio, E., 2009. Nivel relativo del mar en la costa pacífica sur de Colombia: variabilidad, tendencias e implicaciones en la dinámica deltaica. Boletín Geológico 42, 53–66.

Meyer, H., Mejía, J.A., Velásquez, A., 1992. Informe preliminar sobre el terremoto del 19 de noviembre de 1991 en el Departamento del Chocó. Publicaciones Ocasionales OSSO, Universidad del Valle, Cali, Colombia. 13 pp.

Moreno, J.M., 2003. Alvusión de canales en la evolución morfodinámica del delta del río Patía, Colombia. In: Montañez, G., Campos, N., Avella, F., Polanía, J. (Eds.), El mundo marino de Colombia: investigación y desarrollo de territorios olvidados. Universidad Nacional de Colombia Press, Bogotá, Colombia, pp. 121–137.

Morton, R.A., González, J.L., López, G.I., Correa, I.D., 2000. Frequent non-storm washover of barrier islands, Pacific coast of Colombia. Journal of Coastal Research 16, 82–87.

Nittrouer, C.A., Kuehl, S.A., Figueiredo, A.G., Allison, M.A., Sommerfield, C.K., Rine, J.M., Faria, E.C., Silveira, O.M., 1996. The geological record preserved by Amazon shelf sedimentation. Continental Shelf Research 16, 817–841.

Overeem, I., Syvitski, J.P.M., 2009. Dynamics and Vulnerability of Delta Systems. LOICZ Reports & Studies No. 35. GKSS Research Center, Geesthacht. 54 pp.

Pennington, W.D., 1981. Subduction on the eastern Panama Basin and seismotectonics of Northwestern South America. Journal of Geophysical Research 86, 10753–10770.

Quinn, W.H., Zopf, D.O., Short, K.S., Kuo Yang, R.T.W., 1978. Historical trends and statistics of the Southern Oscillation, El Niño, and Indonesian droughts. Fishery Bulletin 76, 663–678.

Restrepo, J.D., Kjerfve, B., 2000. Water discharge and sediment load from the western slopes of the Colombian Andes with focus on Rio San Juan. Journal of Geology 108, 17–33.

Restrepo, J.D., Kjerfve, B., 2002. San Juan River delta, Colombia: tides, circulation, and salt dispersion. Continental Shelf Research 22, 1249–1267.

Restrepo, J.D., Kjerfve, B., Correa, I.D., González, J.L., 2002. Morphodynamics of a high discharge tropical delta, San Juan River, Pacific coast of Colombia. Marine Geology 192, 355–381.

Restrepo, J.D., López, S.A., 2008. Morphodynamics of the Pacific and Caribbean Deltas of Colombia, South America. Journal of South American Earth Sciences 25, 1–21.

Restrepo, J.D., Kettner, A., 2012. Human induced discharge diversion in a tropical delta and its environmental implications: the Patía River, Colombia. Journal of Hydrology 424–425, 124–142.

Soeters, R., Gómez, J., 1985. Contribución del studio geomorfológico para el proyecto de canales y esteros. In: Rizo, D., Contreras, R. (Eds.), Estudio del impacto ambiental para la proyección y canalización de esteros. Corporación Valle del Cauca-Plan de Adecuación de Esteros y Canales, Cali, pp. 285–337.

Storms, J.E.A., Hoogendoorn, R.M., Dam, R.A.C., Hoitink, A.J.F., Kroonenberg, S.B., 2005. Late-Holocene evolution of the Mahakan delta East Kalimantan, Indonesia. Sedimentary Geology 180, 149–166.

Syvitski, J.P.M., Saito, Y., 2007. Morphodynamics of deltas under the influence of humans. Global and Planetary Change 57 (3), 261–282.

Syvitski, J.P.M., Kettner, A.J., Overeem, I., Hutton, E.W.H., Hannon, M.T., Brakenridge, G.R., Day, J., Vorosmarty, C., Saito, Y., Giosan, L., Nicholls, R.J., 2009. Sinking deltas due to human activities. Nature Geoscience 2, 681–686.

Tavera, H.A., 2009. Documentos síntesis. Proyecto caracterización, diagnóstico y zonificación de los manglares en el departamento de Nariño. Ministerio de Ambiente, Vivienda y Desarrollo Territorial, Corporación Autónoma Regional de Nariño y World Wide Found for Nature-WWF Colombia. Bogotá. 50 pp.

Thieler, E.R., Himmelstoss, E.A., Zichichi, J.L., Ergul, A., 2009. Digital Shoreline Analysis System (DSAS) version 4.0—an ArcGIS extension for calculating shoreline change.

U.S. Geological Survey Open-File Report 2008–1278http://pubs.usgs.gov/of/2008/1278/. Available at:.
Thom, B.G., 1967. Mangrove ecology and deltaic geomorphology, Tabasco, Mexico. Journal of Ecology 55, 301–343.
Tolman, H.L., 2002. Validation of WAVEWATCHIII version 1.15 for a global domain. Technical note, National Oceanic and Atmospheric Administration-National Weather Service, Washington, D.C., 33 pp.
Van Es, S., 1975. Análisis geológico de las imágenes de radar de la llanura Pacífica de Nariño, Colombia. Revista CIAF 2, 87–98.
Vann, J., 1959. Landform–vegetation relationships in the Atrato delta. Annals of the Association of American Geographers 49, 345–360.
Velásquez, A., Meyer, H., Marin, W., Ramirez, F., Drews, A.D., Campos, A., Hermelin, M., Bender, S., Arango, M., Serje, J., 1994. Planificación regional del occidente colombiano bajo la consideración de las restricciones por amenazas. Memorias del Taller OEA sobre planificación del desarrollo regional y prevención de desastres, Spec. Publ, pp. 1–36.
West, R.C., 1957. The Pacific Lowlands of Colombia—A Negroid Area of the American Tropics. Louisiana University Press, Baton Rouge. 278 p.
Wright, L.D., Coleman, J.M., 1973. Variations in morphology of major river deltas as functions of ocean wave and river discharge regimes. Bulletin of the American Association of Petrologists and Geologists 57, 370–398.